nature portfolio

Peer Review File

Reaching the Efficiency Limit of Arbitrary Polarization Transformation with Non-orthogonal Metasurfaces

Editorial note: Parts of this Peer Review File have been redacted as indicated to remove third-party material where no permission to publish could be obtained.

REVIEWER COMMENTS

Reviewer #1 (Remarks to the Author):

The manuscript introduces non-orthogonal metasurfaces that can realize any desired input and output polarization conversion with near-unity efficiency. To the best of our knowledge, this is the first demonstration of the conversion of non-orthogonal polarizations. It is important to push the limitation of polarization multiplexing since the one critical bottleneck of the metasurface is its passive nature. The proposed approach for addressing the challenge is novel. Moreover, high efficiency is the most necessary property for a polarization converter if it is used for practical applications. Overall, I think this work will have great promise in polarization multiplexing, communication, and information encryption applications. The manuscript is valuable and well-written. I recommend this work be published in Nature Communications if the authors could address my concerns regarding

1. Multi-layered metasurface can offer numerous advantages from a functional perspective, but they come with drawbacks such as increased complexity in fabrication and design, as well as a larger form factor. While meaningful functions have been demonstrated to mitigate these advantages, I am just curious about potential methods, even through future research, to reduce the number of layers. Is there a way to reduce the number of layers without compromising the demonstrated functions?

2. In a polarization converter, achieving broadband high efficiency is crucial, but accomplishing these properties through a metasurface is known to be challenging. The authors emphasize the significance of achieving broadband high efficiency both in the title and throughout the manuscript. However, a more detailed explanation of how they achieved broadband high efficiency seems necessary. It would be beneficial if the author could provide a more in-depth description, whether it comes from material properties, meta-atom geometry, or other factors.

3. In line with the previous comment, given that high efficiency is one of the main novelties

of this paper, providing a more detailed explanation of how efficiency was measured would be beneficial. In Figure 3e, it appears that there are portions where the measured efficiency exceeds 1. (In my opinion, it might be results from the absence of axis bars which makes the accurate interpretation of axis positions challenging. It would be helpful to include axis bars to indicate the precise locations on the axes for better clarity.

4. In Figure 4c, the holograms don't appear vivid and clear. While high efficiency is expected to enhance the vividness and clarity of the hologram, what could be the reasons for the observed discrepancy? Could you provide insights into the factors that might be contributing to this outcome?

5. The authors may consider the following design approach and remaining challenge references:

https://onlinelibrary.wiley.com/doi/abs/10.1002/adma.202206399

https://www.nature.com/articles/s41377-023-01169-4

Reviewer #2 (Remarks to the Author):

Review for "Reaching the Efficiency Limit of Arbitrary Polarization Transformation with Non-orthogonal Metasurfaces" by Yueyi Yuan et al.

The authors present a numerical and experimental analysis of the possible benefits of metamaterials with inhomogeneous Jones matrices.

The study at the base of the manuscript seems thorough to me and the experimental results support the claims in the manuscript.

While inhomogeneity was examined as a concept before (e.g. by the cited work by Chipman), I find the topic interesting, and, due to its transferability to the optical domain and the current interest in multi-layer metasurfaces, it could also interest a broad readership.

However, in its current form, the main manuscript is inaccessible to a non-specialist (and maybe even a specialist). In contrast, the Supplementary Information can be followed much better.

Summarizing, I believe the manuscript could eventually be published in Nature Communications, however, prior, the presentation requires a rework of the presentation.

Major points:

For publication in a broad audience journal such as Nature Communications, I believe it is necessary to move explanations from the SI to the main manuscript.

The figures present overwhelming amounts of data and the reader is sometimes left to interpret them on their own. Reducing the amount of shown data or expanding the figure captions to guide the reader more would be nice. The figure captions should introduce the symbols used in the figures. Some symbols seem to be unnecessary because they are not treated in the manuscript (e.g., r, wx, wy, FLL, FRL, H). The Poincare spheres in Fig. 4A are hardly discussed.

Some of the plots are indiscernible, e.g. Fig. 2B, Fig. 2C, Fig. 3E.

Fig. 1D: In the experiment, there is considerable S1 and S2 intensity in the output states 1 and 13, even when the simulation says there should be little intensity. For the other states, the simulation fits the experiment quite well. Could this be a background issue? If yes, the other efficiencies should be corrected. If not, a comment would be good.

I believe the experimentalist's understanding would benefit from more comparison with standard polarization components such as waveplates and polarizers.

It would also be nice to have a clear line drawn where the capability of standard optics ends and only metasurfaces can achieve what is presented. I believe this is from line 237, but I can be convinced that this line was overstepped earlier in the manuscript.

The structured spacer layers are not mentioned at all in the manuscript and hardly in the SI. I do not know if they must be structured, or what the function of their structure is.

For certain applications, such as differential detection, very clean polarization states and high extinction factors are necessary. Other applications are forgiving in this respect. A comment on the theoretical limits of using metasurfaces would be nice.

Line 222, Fig 3E, Fig S15, S16: the error/fluctuation periodically reduces to zero. If this observation is correct, I expect a calculation error.

Minor comments

Line 92: the angle symbol is often used and could be introduced at first use.

Line 118: the Coverage Ratio R is typeset in bold, however, to me, it should be a scalar or I misunderstand.

Line 129: Fig. 1E does not exist, maybe the authors mean Fig. 1C.

Line 171: symmetry pattern should be replaced by the exact symmetry necessary.

Line 177: px and py and a are never introduced.

Line 185 and Fig. 3A: would it not be more convincing if the same output states would be chosen for all input states?

Line 208 and Line 234: the RMSE of the same parameters should be given to allow comparison.

Fig. 2E: it is hard to interpret the data in these plots without a reference for baseline and units / 2 pi.

Fig. 3A: the dashed line is hardly visible anywhere, its color could be changed.

Fig 3C: a color plot with a color map reduced to [0.8, 1] would be easier to read.

Fig. 4C: it should be xy plane instead of xoy plane if z is not 0.

Fig. 4D: the data would be more readable if the plot resembled Fig. 3D.

I have not found a picture of the goal intensity profiles of the number-dot holograms.

The spelling of words starting with eigen sometimes uses a dash, a space, or no space. This should be harmonized.

The manuscript lacks some articles, the authors use constrain but I believe it should be constraint.

Reviewer #3 (Remarks to the Author):

The authors introduced a framework to use the non-orthogonality of eigenstate pairs of non-Hermitian Jones matrices to achieve any polarization transformations. They used multilayered metasurfaces to relax the requirement for orthogonality between polarization eigenstates, resulting in efficient and broadband polarization transformations. The capabilities to enable gating and independent modulation in quadplex transmitting channels were also demonstrated. But we have some concerns to be addressed before considering publication.

1. The authors mentioned that non-orthogonal metasurfaces can be used to achieve arbitrary input-output polarization modulations in a broadband and angle-insensitive manner. The authors should explain what "angle-insensitive" means in this context. Does it refer to the incident angle or other angles? It seems that there is no result or data provided to prove that the discussed system is truly angle-insensitive. I suggest the authors to provide more details to support the conclusion of "angle-insensitive manner".

2. The authors should provide more details on the experimental setup of the gating of CP channels and independent hologram manipulations for reproducibility. In addition to considering the phase compensation for the target image, it is necessary to consider the phase difference of incident waves in a metasurface-based hologram. I suggest to clarify if there is a specific angle for the incident wave. Is the incident wave a uniform plane wave or a Gaussian wave? The phase and amplitude spectra of the S parameters for non-orthogonal metasurfaces should also be given, as they are the critical parameters for metasurface-

based hologram.

3. In the measurement of the near-field distributions, a probe was used as the receiver. Generally, a probe can only measure the electrical field at a localized point in space, making it difficult to accurately measure the response of left-handed or right-handed polarized waves. More details should be given to demonstrate how to use the probe to measure the holographic images under different circular polarization excitations and why a circularly polarized horn is not used as the receiving antenna.

4. In Fig. 3E, the measured polarization conversion efficiency of the metasurface samples is very high in the bandwidth of 8 GHz-12 GHz. However, in Figure 4E, why does the bandwidth reduce to 9 GHz-11 GHz?

5. There are many existing orthogonal metasurfaces that can reach a 100% polarization conversion efficiency in a wide bandwidth, such as PB-phase metasurfaces. The authors should further discuss the performances or functionalities that cannot be achieved by these orthogonal metasurfaces but can be offered by the proposed non-orthogonal metasurfaces.

Other minor concerns:

Line 57, "the center (7))" should be corrected to "the center (7)"

Line 253, "selected threshold as $|F| > 0.7$ and suppressed threshold as $|F| < 0.1$," please give the definition of $|F|$.

Line 264, "Under normal illumination of LHCP or RHCP beams propagating along +z-axis," please add the corresponding Cartesian coordinate in Fig. 4B.

The resolution of figures is a bit low, please improve them.

Reviewer #4 (Remarks to the Author):

I co-reviewed this manuscript with one of the reviewers who provided the listed reports. This is part of the Nature Communications initiative to facilitate training in peer review and to provide appropriate recognition for Early Career Researchers who co-review manuscripts.

Comments from Reviewer #1:

General comment: The manuscript introduces non-orthogonal metasurfaces that can realize any desired input and output polarization conversion with near-unity efficiency. **To the best of our knowledge, this is the first demonstration of the conversion of non-orthogonal polarizations. It is important to push the limitation of polarization multiplexing since the one critical bottleneck of the metasurface is its passive nature**. The proposed approach for addressing the challenge is **novel**. Moreover, high efficiency is the most necessary property for a polarization converter if it is used for practical applications. Overall, **I think this work will have great promise** in polarization multiplexing, communication, and information encryption applications. The manuscript is **valuable and well-written**. I recommend this work be published in Nature Communications if the authors could address my concerns regarding:

Response: We are grateful for the positive feedback of our work. The paper has been revised following your constructive comments and suggestions. Hope the revised version would indeed contribute to the polarization multiplexing field.

Comment: 1. Multi-layered metasurface can offer numerous advantages from a functional perspective, but they come with drawbacks such as increased complexity in fabrication and design, as well as a larger form factor. While meaningful functions have been demonstrated to mitigate these advantages, I am just curious about potential methods, even through future research, to reduce the number of layers. Is there a way to reduce the number of layers without compromising the demonstrated functions?

Response: Actually, the answer to this question is "Yes", there exists a replaceable method to reduce the number of layers while maintaining the demonstrated function. The most important contribution in our work is the underlying relationship between non-orthogonal eigen-vectors and transformation efficiency of arbitrary input-output elliptical polarizations. That is to say, the full capacity of non-orthogonality between two eigen-vectors is the primary condition to approach the efficiency limit, which can be described by the degree of inhomogeneity $|\eta|$ with coverage of [0, 1]. As demonstration, we exploited a meta-atom configuration composed of functional birefringent rectangular patch elements with i (i = 1, 2, 3, 4) layers stacking. The corresponding simulated inhomogeneity degree against rotating bottom patch element from 0° to 180° are shown in Fig. R1a (Fig. S8a in supplementary information). We found that the minimum stacking layers of such birefringent patches to full coverage of $|\eta|$ is ***three***. Additionally, to explore simplified and universal metasurface platform, we have theoretically derived that the minimum number of stacking functional elements to obtain $|\eta| \in [0,1]$ is also related with the in-plane complexity of the meta-atom. We have established a representative meta-atom whose functional element is an anisotropic pattern like L-shape. Fig. R1b (Fig. S8b in supplementary information) displays the simulated inhomogeneity degree of meta-atoms with stacking i (i = 1, 2, 3, 4) layers of the L-shaped elements. We can see that the effective $|\eta| \in [0,1]$ can be obtained by double-layer configuration. That is to say, the minimum stacking number, when using anisotropic meta-elements, can be decreased to only ***two***, which is in agreement with our theoretical derivations. Meanwhile, the non-orthogonal eigen-state pairs and corresponding near-unity efficiency performances are also conducted and verified in both optical region (wavelength 600 nm) and microwave region (wavelength 30 mm), as specifically shown in Note 5 and Note 9 of the revised supplementary information.

To conclude, although multi-layered meta-atom with stacking three functional elements as the implementation platform is adopted in this manuscript, **we also verified that to achieve the required high-efficient polarization conversion, the minimum number of stacking layers can be reduced to two by adopting anisotropic-shaped elements.** This would powerfully support the developments and applications of our proposed scheme.

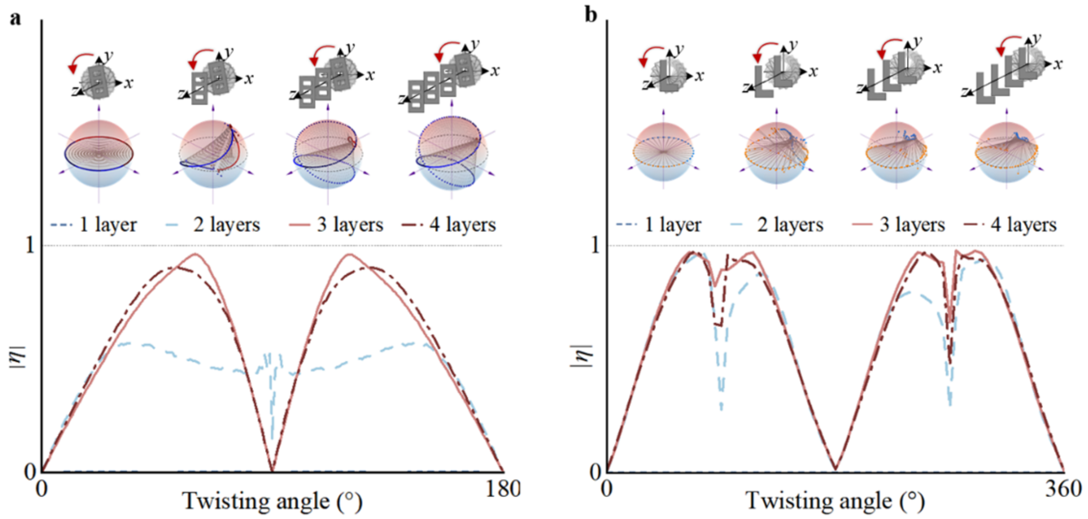

Fig. R1 (Fig. S8 in revised supplementary information) Verifications of inhomogeneity degrees for different meta-atom configurations. Degree of inhomogeneity profiles of meta-atom with stacking i = 1, 2, 3, 4 layers of (a) rectangular patches against rotation of the bottom layer from 0° to 180°, and (b) "L"-shaped elements against rotation of the bottom layer from 0° to 360°. The insets show the simplified schematic of meta-atom with distinct layers of (a) rectangular patch and (b) "L"-shaped elements, and the corresponding evolution trajectories of eigen-state pairs on the Poincaré sphere.

Revisions in manuscript:

The relationship between stacking number of functional elements and its in-plane complexity is re-emphasized in **line 155 – 159** in the revised manuscript.

Revisions in supplement information:

The analyses and simulation verifications on the minimum number of stacking anisotropic L-shaped elements have been added in **Note 5 and Note 9** in the revised supplementary information.

Comment: 2. In a polarization converter, achieving broadband high efficiency is crucial, but accomplishing these properties through a metasurface is known to be challenging. The authors emphasize the significance of achieving broadband high efficiency both in the title and throughout the manuscript. However, a more detailed explanation of how they achieved broadband high efficiency seems necessary. It would be beneficial if the author could provide a more in-depth description, whether it comes from material properties, meta-atom geometry, or other factors.

Response: We thank the reviewer for giving us an opportunity to re-clarify the underlying principle of arbitrary polarization transformation with near-unity efficiency. **Overall, reaching efficiency limit of arbitrary polarization conversion is achieved by adopting non-orthogonal eigen formalism, while the broadband performance is realized by adopted multi-layered meta-atom with non-resonant configuration in microwave region.** Specifically, the in-depth description of both high efficiency and broadband properties are illustrated separately as follows:

(i) *High efficiency from the mechanism view*: a two-order complex Jones matrix can be adopted to describe the polarization tuning ability of the corresponding optical device or medias, whose eigen-values and eigen-vectors directly determine the target polarization behaviors. When input and output polarization states are fixed, the transformation and transmission performances of polarization conversion process totally depend on the matching degree between target input-output combination and the Jones matrix of optical / microwave device. In the most general cases, when we consider either a classical birefringent material or a single layer metasurface, the corresponding eigen-vectors are orthogonal, leading to the limited matching capability to arbitrary elliptical input-output polarization conversion. This orthogonality constraint introduces imperfect matching for arbitrary elliptical conversion in full polarization space, as we have numerically demonstrated in the main text as Fig. 1C and 1D. Instead, non-orthogonal eigen formalism shown herein to provide sufficient degree of freedoms to achieve abundant matching Jones matrix models. After establishing the analytical relationship between non-orthogonality and polarization conversion efficiency, we have implemented the non-orthogonal Jones matrix scheme using multi-layered metasurfaces and have validated their near-unity efficiency performances with representative elliptical polarization conversion experiments.

(ii) *Broad bandwidth from the performance view*: the proposed meta-atom configuration has been designed using five cascaded metallic layers, including three patch elements and two grid-mesh elements. These elements are placed in an interleaved manner. Different with the resonant meta-atom, the non-resonant multi-layered meta-atom can be effectively regarded as a multi-level filter, which exhibits broadband characteristic, associated with a smooth spectral phase change. The simulated complex eigen-values of a representative meta-atom have been presented in Fig. 2E, verifying the element's broadband performance. In order to match the pre-set input-output polarization states, the adopted meta-atom configurations with non-orthogonal eigen formalism are evaluated. The measured efficiency of target input-output conversion within bandwidth is displayed in Fig. S15, which can reach unity at the center frequency of 10 GHz. Due to the unavoidable dispersion effect, at least for basic meta-atom design, the output polarization does vary with frequency in the operating bandwidth (from 8 GHz to 12 GHz) for a fixed input state. Thus, the output energy distributed in the target output polarization state would be slightly reduced compared to the one at the center frequency, as exhibited in Fig. S16. Even so, the bandwidth performances can still prove the achievability and feasibility of our proposed non-orthogonal metasurface for arbitrary polarization conversions with extremely high efficiency. Further refinements, for example inspired by the previous work in the metasurface community on dispersion-engineering, could be considered to improve the device bandwidth.

Revisions in manuscript:

(i) The physics associated to the arbitrary polarization transformation efficiency has been added in **line 47 - 51**, and the underlying principle of our proposed non-orthogonal eigen-formalism for achieving such near-unity efficiency has also been explained in **line 62 – 70** , expressed by **Eq. (2)** , and numerically verified in **Fig. 1C and 1D** in the revised manuscript.

(ii) The polarization transformation and transmission efficiencies within the working band have been experimentally re-measured as shown in **Fig. 3E**, and the corresponding polarization dispersion effect mentioned in the comment has been introduced in **line 239 – 246** in the revised manuscript.

Revisions in supplement information:

The broadband performance relies on the proposed multi-layered non-resonant meta-atom that is designed according to the effective filtering theory in the microwave region, as added in **Note 4** in the revised supplementary information.

Comment: 3. In line with the previous comment, given that high efficiency is one of the main novelties of this paper, providing a more detailed explanation of how efficiency was measured would be beneficial. In Figure 3e, it appears that there are portions where the measured efficiency exceeds 1. (In my opinion, it might be results from the absence of axis bars which makes the accurate interpretation of axis positions challenging. It would be helpful to include axis bars to indicate the precise locations on the axes for better clarity.

Response: We are grateful for the reviewer and we would like to detail the measurement methods of efficiency and explain the ambiguities in Fig. 3E.

(i) *Measurement methods of efficiency*.

Theoretically, the efficiency of the elliptical input-output polarization conversion is calculated by $T = \frac{\langle E^{out} | E^{out} \rangle}{\langle E^{in} | E^{in} \rangle} = \frac{\langle E^{in} | \boldsymbol{J}^{\dagger}\boldsymbol{J} | E^{in} \rangle}{\langle E^{in} | E^{in} \rangle}$, where $\boldsymbol{J} = \begin{bmatrix} J_{xx} & J_{xy} \\ J_{yx} & J_{yy} \end{bmatrix}$ is equivalently considered as the measured scattering complex coefficients of the metasurface sample. We see that when input state $|E^{in}\rangle$ is fixed, the measured efficiency of arbitrary polarization conversion can be calculated by the complex scattering matrix in transmission mode *J*. Thus, it is important to obtain the measured scattering matrix $\boldsymbol{J}$ with quadruplex complex coefficients in linear polarization base. The scattering parameter measurements in microwave region are conducted in an anechoic chamber, and the experimental setup is schematically illustrated in Fig. S14A. To fully obtain transmission coefficients J_{xx}, J_{xy}, J_{yx}, J_{yy}, we used dual-polarized horn antennas as both transmitting and receiving end, and through set them under horizontal and vertical modes to emit and receive *x*- and *y*-linearly polarized electric fields, respectively. Herein, the vector network analyzer (VNA) is used to collect the complex scattering parameters. Consequently, the quadruplex transmission field components in linear polarization base can be measured and used to form the matrix $\boldsymbol{J}$. Thereafter, the measured efficiency of the input-output polarization conversion can be obtained, and the additional eigen-states and eigen-values of matrix $\boldsymbol{J}$ can be fully calculated. The transmission coefficient under the same experimental setup without interposing along the beam path any fabricated metasurface is used as the normalization standard.

(ii) *Ambiguities in Fig. 3E.*

In the previous version of manuscript, Fig. 3E displays the measured efficiency profiles of three representative metasurface samples within bandwidth 8 GHz – 12 GHz. The solid curves are the measured efficiencies and labelled shadows around the curves denotes the fluctuations during the measurement process. As mentioned by the reviewer, it seems that parts of the curves exceed 1, but this was due to the way we plotted our curves, without the axis bars. To address the referee concern and clarify this experiment, we have re-measured all of the three samples and have added the error bars, associated to each measurement, to label the accurate efficiency values, as displayed in Fig. R2.

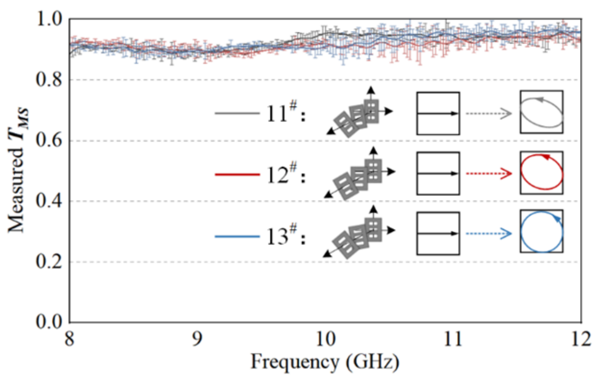

Fig. R2 (Fig. 3E in revised manuscript) Measured efficiency within the bandwidth of 8 GHz – 12 GHz for 11#, 12#, 13# samples. The error bars present the corresponding noisy fluctuations in the measurement processes, and the insets present the schematic of meta-atom configurations and the target input (left) – output (right) polarization conversions.

Revisions in manuscript and supplementary information:

(i) The measurement setup and efficiency analyses for arbitrary input-output polarization conversion has been mentioned in **lines 213 - 214** in the revised manuscript and specifically detailed in **Note 7.3** in the revised supplementary information.

(ii) The ambiguities in measured efficiency profiles have been corrected after **re-measuring** the response of the three metasurface samples and re-organized the data using error bars in **Fig. 3E** in the revised manuscript and **Fig. S15 and S16** in the revised supplementary information.

Comment: 4. In Figure 4c, the holograms don't appear vivid and clear. While high efficiency is expected to enhance the vividness and clarity of the hologram, what could be the reasons for the observed discrepancy? Could you provide insights into the factors that might be contributing to this outcome?

Response: We thank the reviewer for this meaningful comment. The reasons for which the holograms do not appear as vivid as expected by the referee are due to the following three aspects.

(i) *In mechanism*: although near-unity efficiency for arbitrary input-output polarization conversion is obtained considering a single input to a single output channel, when multiple polarization channels are utilized simultaneously (multiple inputs to multiple outputs), the transmitted output energy must be distributed into each modulated polarization component. Thus, the efficiency in each selected circularly polarized channel is divided by the number of channels, in strong comparison with the scenario when only one channel is selected, as illustrated in Fig. 4D. This means that the image quality of holograms, using more than one channels projection scheme, would be inevitably degraded the image vividness due to the polarization multiplexing.

(ii) *In design*: limited holographic resolutions and vividness primarily originate from the non-ideal phase responses of the adopted meta-atoms for the metasurface construction. In our work, each non-orthogonal metasurface sample is composed of 31 × 31 meta-atoms, which should satisfy the required discretized phase distributions in all multiplexed polarization channels, and are simultaneously constrained by the required channel gating effects. If more than one routed CP channel is considered, then the phase profiles, each associated to a given CP channel, are needed. Therefore, each phase profile of a given CP channel has to be chosen by compromising the available phase resources on the other channels. The resolution of reconstructed patterns in the different channels would accordingly be affected, restricting the image projection quality of each channel. Meanwhile, the discontinuous phase distributions contribute to the unpredictable interferences around focusing points in target holographic pattern, which would inherently affect the imaging quality.

(iii) *In experiment*: the near-field mapping experiment is conducted in an anechoic chamber, but there still exist unavoidable interferences, diffractions, and noises. Our transmitting source is emitted from a horn antenna and it is designed to launch the required LHCP or RHCP plane waves. In our experiment, the propagating distance between transmitting antenna and metalens is more than $20\lambda_0$, so that the incident wavefronts can be regarded as quasi-plane waves. However, the effects of practical spherical wavefronts still cannot be totally eliminated, and the phase discrepancy between the middle and edge of metasurface would further affect the output hologram fields. As the beam would exhibits unavoidable expansion during propagating, and due to the finite surrounding absorbing materials around the fabricated sample, as shown in Fig. S14B in SI, complex interferences on the imaging plane could occur. Also, the receiver probe is driven by a motion controller, which would introduce minute mechanical vibration during measurement, disturbing the collected electric field information and introducing inevitable noises in holograms.

To conclude, the qualities of measured holograms are limited due to the mechanism used for projection, the hologram design themselves, and the uncertainties in the experimental setup. Imaging resolution can be enhanced by exploiting neural-network based amplitude-phase imaging algorithm and optimizing measurement schemes. Although there exist some imperfections in the proof-of-concept demonstration of multiplexed holograms, the feasibility of the proposed non-orthogonal eigen formalism and its potentials in reaching the efficiency limit have been validated. We thank reviewer again for this valuable comment and we have added these discussions on the quality of the produced holograms in the revised manuscript.

Revisions in manuscript and supplementary information:

We have mentioned a brief explanation on the quality of the produced holograms in lines **293 – 295** in the revised manuscript and specifically analyzed its originalities as detailed in **Note 10.6** in the revised supplementary information.

Comment: 5. The authors may consider the following design approach and remaining challenge references:

https://onlinelibrary.wiley.com/doi/abs/10.1002/adma.202206399

https://www.nature.com/articles/s41377-023-01169-4

Response: We are grateful for reviewer to provide these valuable works on metasurface. We have carefully studied these works and found that they have great significance to broaden and supplement our introduction part. In [*Advanced Materials, 2023, 35, 2206399*], the authors systematically revisited the design approaches for conventional and unconventional metasurfaces, including the basic principle of scalar diffraction theory, multi-dimensional degree of freedoms utilization of unit cell, and versatile functionalities modulation methods. This comprehensive review work can powerfully support the background investigation of metasurface construction strategies, and is added as Ref. [13] in the revised manuscript. In [*Light: Science & Applications, 2023 12, 152*], the authors summarized the advanced applications based on integration metasurfaces, inspired by hybridization with various optical components and photonics devices. They deeply analyzed the challenging and prospects of integrated metasurfaces in the future photonic platform. This work is quite valuable to help us broaden the application background of metasurface studies, and validate the necessity of full-band expansion of our proposed high-efficiency scheme. We have added this paper as Ref. [14] in the revised manuscript.

Revisions in manuscript:

We have added these two works as **Ref. [13] and [14]** in the revised manuscript.

Reviewer #2 (Remarks to the Author):

General comment: Review for "Reaching the Efficiency Limit of Arbitrary Polarization Transformation with Non-orthogonal Metasurfaces" by Yueyi Yuan et al.

The authors present a numerical and experimental analysis of the possible benefits of metamaterials with inhomogeneous Jones matrices. The study at the base of the manuscript **seems thorough to me** and the experimental results support the claims in the manuscript. While inhomogeneity was examined as a concept before (e.g. by the cited work by Chipman), **I find the topic interesting, and, due to its transferability to the optical domain and the current interest in multi-layer metasurfaces, it could also interest a broad readership**. However, in its current form, the main manuscript is inaccessible to a non-specialist (and maybe even a specialist). In contrast, the Supplementary Information can be followed much better. Summarizing, I believe the manuscript could eventually be published in Nature Communications, however, prior, the presentation requires a rework of the presentation.

Response: We thank the reviewer for the positive evaluations on our work. According to the detailed suggestions, we have made extensive corrections in our manuscript, as listed below.

Major points:

Comment: (1) For publication in a broad audience journal such as Nature Communications, I believe it is necessary to move explanations from the SI to the main manuscript.

Response: We thank the reviewer for this constructive suggestion. In this work, we aim to propose a general scheme for reaching efficiency limit of arbitrary polarization conversion by adopting metasurface with non-orthogonal eigen-formalism, and the key factor is to reveal the underlying relationship between non-orthogonality of eigen-states and arbitrary polarization transformation efficiency, which is detailed along with the derivation processes including principles and explanations of eigen-formalism and bi-orthogonal system. In the previous version, the corresponding derivation process in the main text is somewhat simplified. As mentioned by reviewer, final expressions of transformation efficiency exhibited in main text is not readable for broad audiences. Following the comment, we have re-organized the theory part and supplemented primary derivation steps and definitions logically in the revised main text.

Revisions in manuscript:

We have moved part of the eigen-derivations from SI to the **revised main text in lines 88 – 101**.

Comment: (2) The figures present overwhelming amounts of data and the reader is sometimes left to interpret them on their own. Reducing the amount of shown data or expanding the figure captions to guide the reader more would be nice. The figure captions should introduce the symbols used in the figures. Some symbols seem to be unnecessary because they are not treated in the manuscript (e.g., r, wx, wy, FLL, FRL, H). The Poincaré spheres in Fig. 4A are hardly discussed.

Response: We thank for these detailed suggestions and we would like to reply them one by one.

(i) *The overwhelming amounts of data in figures.*

In our previous manuscript, each figure with several sub-figures or insets contains a lot of data, and the corresponding captions indeed just illustrated some primary information. As suggested by reviewer, we have supplemented the specific illustrations of each symbol and annotations. Meanwhile, we have removed some irrelevant information from the figures.

(ii) *Unnecessary symbols in the manuscript (e.g., r, wx, wy, FLL, FRL, H)*.

As suggested by the reviewer, we have moved the whole introduction of geometric meta-atom configuration to supplementary information and just exhibit a schematic of structure topology in Fig. 2. Thus, we have deleted parameters r, w_x, w_y, in the revised main text and figure. Meanwhile, F_{LL} and F_{RL} are important symbols for further illustration of channel gating and multiplexing demonstrations. So we have added the specific explanations of these coefficients. Besides, thickness H is also a primary information of the fabricated sample. Therefore, we have added the corresponding explanation in the revised main text and caption of Fig. 4B. We have also carefully re-checked all of the other symbols in the manuscript, to guarantee that all mentioned ones are illustrated.

(iii) *Lacking analyses on Poincaré spheres in Fig. 4A.*

Poincaré spheres in Fig. 4A illustrate the eigen-states distributions of Jones matrices changing with different selection effects. For instance, the 1st schematic in Fig. 4A shows the function of $\boldsymbol{C}_4^1$ gating effect of L-L channel while suppressing other three channels (R-L, L-R, and R-R). Such gating condition requires four transmission coefficients in inhomogeneous Jones matrices to be $|F_{LL}| \to 1$, $|F_{RL}| \to 0$, $|F_{LR}| \to 0$, $|F_{RR}| \to 0$, and the eigen-vectors in polarization space are correspondingly displayed on the Poincaré sphere. We can see in this $\boldsymbol{C}_4^1$ case, eigen-vector pairs are distributed around north and south pole. This indicates that such single-channel gating effect can be guaranteed by quasi circular eigen-polarizations. As for $\boldsymbol{C}_4^2$ gating of L-L and R-L channels shown in the 2nd schematic in Fig. 4A, corresponding eigen-vectors distributions on Poincaré sphere change with the condition of Jones matrices to be $|F_{LL}| \to 1$, $|F_{RL}| \to 1$, $|F_{LR}| \to 0$, $|F_{RR}| \to 0$. The eigen-vector pairs are distributed separately with one around north pole and the others near the equator, and they are obviously non-orthogonal to each other. Similarly, the conditions of inhomogeneous Jones matrices with $\boldsymbol{C}_4^3$ and $\boldsymbol{C}_4^4$ gating effects are schematically presented in Fig. 4A. Increasing the number of gated channels results in eigen-vector pairs uniformly distributed on the Poincaré sphere, further demonstrating the non-orthogonality. This polarization multiplexing demonstration not only verifies the potential of non-orthogonal eigen-formalism, we also used it to independently address phase modulations on each of the transmitted channel. The related primary information and explanations with Poincaré sphere in Fig. 4A have been added in the revised manuscript.

Revisions in manuscript:

(i) We have supplemented **the captions of Fig. 1A, Fig. 1D, Fig. 2A, Fig. 2E, Fig. 4A, and Fig. 4B** in the revised manuscript.

(ii) We have removed some unnecessary symbols, including p_x, p_y, w_x, w_y, r, in **Fig. 2A** in the revised manuscript, and specifically introduced the geometric parameters of meta-atom in revised Note 4 in the supplementary information.

(iii) We have specifically explained implications some important symbols, including ***H* in Fig. 4B**, circularly polarized transmission coefficients F (containing F_{LL} and F_{RL}) in the **lines 270 – 274** in the revised manuscript.

(iv) We have added the analyses on Poincaré sphere in **caption of Fig. 4A** and **lines 278 - 287** in the revised manuscript.

Comment: (3) Some of the plots are indiscernible, e.g. Fig. 2B, Fig. 2C, Fig. 3E.

Response: Thank the reviewer for this kindly reminder, and we are grateful to have a chance to supplement and clarify the explanations on ambiguous figures one by one.

(i) *Fig. 2B and Fig. 2C.*

These two sub-figures exhibit the mappings and tendencies of eigen-vector pairs in term of Jones vectors $\left| \cos\alpha \quad \sin\alpha \cdot e^{i\beta} \right\rangle$, which are tailored by different twisting angles θ_1, θ_2, and θ_3 of the three stacking patch elements in the meta-atom. As mentioned by the reviewer, the previous plots are difficult to distinguish. Thus, we have re-organized Fig. 2B and Fig. 2C in form of two-dimensional contour plots. For all mappings in sub-figures, the axes show θ_2 and θ_3 $\in [0°, 180°]$, and colormaps indicate the tendencies of the target variables α_1, α_2, β_1, β_2, $\Sigma\alpha_i$ and $\Delta\beta_i$, respectively.

(ii) *Fig. 3E.*

Besides, Fig. 3E displays the measured efficiencies of three representative metasurfaces designed to achieve different input-output polarization transformations. To present the results in an intuitive and readable way, we have adopted error bars instead of shadows to illustrate the disturbances and errors of this practical measured efficiency performances. We thank reviewer for this comment again, and we have added the specific explanations of these sub-figures in the revised manuscript.

Revisions in manuscript:

We have specifically explained Fig. 2B and 2C in captions and **lines 170 – 180**, and clarified Fig. 3E in **lines 239 – 246** in the revised manuscript.

Comment: (4) Fig. 1D: In the experiment, there is considerable S1 and S2 intensity in the output states 1 and 13, even when the simulation says there should be little intensity. For the other states, the simulation fits the experiment quite well. Could this be a background issue? If yes, the other efficiencies should be corrected. If not, a comment would be good.

Response: Considering "*S1 and S2 intensity in the output states 1 and 13 in experiment*" in this comment, we think the reviewer means Fig. 3D instead of Fig. 1D. We would like to explain the deviations in calculated, simulated, and measured S1 and S2 intensities for output states 1 and 13.

As for cases 1 and 13, they represent left- and right-handed circular polarization in output fields, whose theoretical Stokes parameters are (0, 0, +1) and (0, 0, -1). Meanwhile, the simulated Stokes parameters of case 1 and 13 are (0.11, -0.07, -0.99) and (0.02, -0.04, 0.99), respectively. As mentioned by the reviewer, there exist some deviations between ideal and simulation results. It is worth noting that the ideal pre-settings are purely numerical, while the simulated input - output polarization conversion processes are obtained using the constructed metasurface model. The simulated metasurface model is composed of 15 × 15 meta-atoms, essentially similar to the fabricated samples. Due to the finite size of the metasurface, it does not correspond to the infinite unit-cell period boundary condition used numerically to calculate the response of the system with full wave simulation. As result, we expect some deviations from the pre-settings desired from the ab-initio calculation. Additionally, the measured Stokes parameters of case 1 and 13 are (0.06, -0.05, -0.99) and (0.09, -0.1, 0.99), respectively. Working with microwaves, we had to use horn antennas at both the transmitting and receiving end, and the measured errors might be caused by the diffraction at the horn apertures. Nevertheless, although there exist some deviations in simulated and measured Stokes parameters from theoretical settings of case 1 and 13, we conclude that the output polarization states can still be maintained to the north or south pole on Poincaré sphere. We want to thank the reviewer again for this comment, and we have supplemented the explanations for these errors in cases 1 and 13 in the revised manuscript.

Revisions in manuscript:

We have explained and analyzed the deviations in S_1 and S_2 of case 1 and 13 in both simulation and measurement results, as added in **lines 228 – 231** in the revised manuscript.

Comment: (5) I believe the experimentalist's understanding would benefit from more comparison with standard polarization components such as waveplates and polarizers.

Response: We are grateful for this advice on comparing standard polarization devices and our proposed non-orthogonal metasurface. Here, we would like to list the related information including configuration, volume, principles, and functionalities. Obviously, the volumes of standard optical polarization components, including but not limited to waveplates and polarizers, are usually bulky compared to the operation wavelengths, and the functionalities are fixed. As for complex polarization manipulation, such as polarized beam steering and filtering, different components need to be cascaded along the optical systems to achieve the required functionalities. Meanwhile, metasurfaces owning miniaturized volumes can support versatile polarization manipulation abilities with high performances. As for our proposed non-orthogonal metasurface scheme, arbitrary polarization conversion can be conducted with near-unity efficiency, and polarization filtering with precise phase modulation can be achieved with customized multiplexing effect.

Table. R1 Comparisons between standard polarization components and our non-orthogonal metasurfaces

	Types	**Configurations**	**Volume**	**Principles**	**Functionalities**
Standard polarization components	Waveplates ($\lambda/2$, $\lambda/4$)	[figure redacted]	$>> \lambda_0$	Birefringent materials with phase	Linear-linear, linear-circular polarization

				retardators	conversion
	Polarizers	**[figure redacted]**	$\gg \lambda_0$	Polarization rotation and filtering	Polarization filtering
	Gratings	**[figure redacted]** Appl. Opt. 50, 2062-2068 (2021)	$\gg \lambda_0$	Periodic spatial diffraction	Polarization diffraction and separation
	Cascading system	**[figure redacted]** Appl. Opt. 46, 6700-6709 (2007)	$\gg \lambda_0$	Multiple optical elements cascaded along the beam path	Nondepolarizing polarization conversion
Our non-orthogonal metasurface		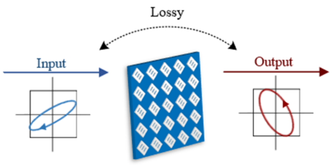	$\ll \lambda_0$	Non-orthogonal eigen-formalism	1. Arbitrary polarization conversion 2. Customized polarization filtering 3. Precise phase-front modulation

Comment: (6) It would also be nice to have a clear line drawn where the capability of standard optics ends and only metasurfaces can achieve what is presented. I believe this is from line 237, but I can be convinced that this line was overstepped earlier in the manuscript.

Response: We thank the reviewer for this suggestion. As in the response to last comment, we have compared the polarization modulation capabilities of standard components and metasurfaces. Actually, we think there exist some limitations of standard optics:

(i) *From functions view:* individual optical element can only produce simple conversion effect on regular linear or circular polarizations. When referred to arbitrary input to arbitrary output elliptical polarizations that are potentially applicable for spectrometer and full-stokes imaging techniques, the conversion or filtering functions would be conducted by multiple-cascading waveplates and polarizers, hindering the miniaturization and integration for applications.

(ii) *From performances view:* although single optical element can obtain linear/circular - linear/circular polarization conversion with high performances, there are very few experiments have been conducted demonstrating polarization arbitrariness, high efficiency, and broad bandwidth properties of elliptical input-output polarization conversion.

(iii) *From potentials view:* classic optical waveplates or polarizers cannot conduct, in addition to the polarization conversion, localized phase-front modulation in sub-wavelength scale, which has shown great potentials in applications of beam-shaping, holographic imaging, cryptography, and so forth.

Thus, we think **the capability of standard optics ends up with the compact integration volumes,**

arbitrary elliptical polarization regulations, and precise phase-front modulations. By contrast, our results not only demonstrate how non-orthogonal metasuface can enhance the polarization modulation regulation capabilities and performances beyond standard optics, while preserving phase modulation potentials and holographic imaging applications of conventional metasurface.

Revisions in manuscript:

We have mentioned the comparison between optical standard elements that belongs to orthogonal devices in **lines 56 – 59** in the revised manuscript.

Comment: (7) The structured spacer layers are not mentioned at all in the manuscript and hardly in the SI. I do not know if they must be structured, or what the function of their structure is.

Response: We thank the reviewer for this valuable comment about the structured spacer layers in our proposed meta-atom configuration. Here we considere the mentioned "*structured spacer layers*" by reviewer as the adopted dielectric substrates on which are printed the meta-atoms, as shown in blue in Fig. 2A. Thus, the answer to the necessity of the structured spacer layers is "Yes, they are indeed needed". From the view of operation scheme, the whole meta-atom structure can be regarded as a cascading network according to the effective microwave filter. The metallic patch and grid patterns operate as capacitive and inductive elements to produce the multiple level LC filter, and the substrate layers are considered as the transmission line, playing a key role in circuit matching for the equivalent circuit model. From the view of design consideration, the substrate material is adopted by polyfluortetraethylene dielectric-slabs with permittivity ε_r = 3.5 and thickness h = 1 mm. There are four pieces of same substrate layers that are designed to support and space the metallic patch- and grid-elements. Note that since the dielectric layer acts as transmission line, we do not need curving the dielectric into specific pattern. As suggested by reviewer, we have added the corresponding explanations on this substrate layers in the revised supplementary information.

Revisions in manuscript:

We have explained the necessity and function of proposed structured spacer layers, as added in **Note 4** in revised supplementary information.

Comment: (8) For certain applications, such as differential detection, very clean polarization states and high extinction factors are necessary. Other applications are forgiving in this respect. A comment on the theoretical limits of using metasurfaces would be nice.

Response: We thank the reviewer for this meaningful comment. The referee is asking a very delicate but also intriguing question about the theoretical limitation of metasurfaces for achieving extremely clean polarization control. It should be noted that several factors are limiting the performance of metasurface in general, not only for polarization modulation. These are nearfield coupling between adjacent elements, fabrication imperfection and accuracy of the modelling and design tool. If these factors can be improved using dedicated approaches, including iterative optimization methods, machine learning and so forth, efficiency barely approached 95%. Note that working at microwave is advantageous to reduce fabrication imperfections. To avoid mentioning improper and potentially controversial statements, we prefer not to engage further in this complex subject. We believe that the question is nevertheless critical for metasurface industrialization and achieving real world impact. We also believe that the question cannot be simply addressed with current stage of the technology development, more dedicated and certainly expensive engineering works are still needed to fully address and settle the point asked by the referee. We hope that the referee could understand our point of view and could appreciate the difficulty in coming up with a definitive statement that would answer this tantalizing question.

Comment: (9) Line 222, Fig 3E, Fig S15, S16: the error/fluctuation periodically reduces to zero. If this observation is correct, I expect a calculation error.

Response: We are grateful to the reviewer about this comment. Actually, in the previous version of Fig. 3E, Fig. S15, Fig. S16, the observation of *error/fluctuation that periodically reduces to zero* is misunderstood by the shadow representation, which is not a profitable / intuitive method to express the practical deviations in the measurement. Thus, to exhibit the efficiency of metasurface samples in a direct and clear manner, we have re-conducted the measurements in microwave anechoic chamber and the results are illustrated in Fig 3E, Fig S15 and Fig S16 with axis bars to label *the errors and fluctuations*, where we can see that the noises and fluctuations are obviously optimized.

Revisions in manuscript:

We have re-measured the polarization conversion efficiencies of these three metasurface samples, and re-organized the efficiency performances in forms of diagrams with **error bars in Fig. 3E** in revised manuscript, and **Fig. S15 and S16** in revised supplementary information.

Minor comments

Comment: (1) Line 92: the angle symbol is often used and could be introduced at first use.

Response: Thank you for this kindly reminder. We have added the explanation of this angle symbol at the first appearance, and checked all other symbols that have been illustrated at the first time in the revised manuscript.

Comment: (2) Line 118: the Coverage Ratio R is typeset in bold, however, to me, it should be a scalar or I misunderstand.

Response: Thank you very much for pointing out this mistake. You are indeed totally correct. The coverage ratio R is a scalar parameter and should be labelled in plain. We have changed typeset of R in revised manuscript.

Comment: (3) Line 129: Fig. 1E does not exist, maybe the authors mean Fig. 1C.

Response: We have revised this labelling mistake in serial number of sub-figure, and re-checked all other labels in figures.

Comment: (4) Line 171: symmetry pattern should be replaced by the exact symmetry necessary.

Response: Thank you for this valuable suggestion. We have specifically described the different symmetric meta-atom patterns and corresponding eigen-modes in the revised manuscript.

Comment: (5) Line 177: px and py and a are never introduced.

Response: We are grateful for this reminder. As mentioned by reviewer, and corresponding to major comment 2 above, we have explained all the specific symbols of meta-atom configuration to the Note 4 in revised SI.

Comment: (6) Line 185 and Fig. 3A: would it not be more convincing if the same output states would be chosen for all input states?

Response: Thank you for this suggestion about the more convincing demonstration of multiple-input-to-single-output polarization transformations. In the part for validating arbitrary polarization transformations, we have proposed 8 × 13 pairs of input-output polarization combinations, i.e., there are 8 different polarizations selected as the input state, and they are preset to transform into 13 different output polarization states, respectively. As shown in Fig. 3A, each row in the chart contains 13 polarization states as the output, while they originate from 8 different input polarization states. This can be regarded as a demonstration for "*the same output states chosen for all input states*". Besides, we also proposed a corresponding demonstration of *Variable input states to fixed output state*, as illustrated in section 8.3 of SI. In this part, we optionally sample 48 representative input elliptical polarization states along a free trajectory on the Poincaré sphere, and set output state fixed as RHCP state. To implement such multiple input to single output process, we employed 48 non-orthogonal metasurfaces with profitable eigen-state pairs. The polarization transformation accuracy, described by RMSE, is about 5.4°, and the efficiency can reach 97%.

As suggested by the reviewer, we have added corresponding conclusions about this *multiple input to single output polarization transformations* in revised manuscript to enhance the convincing of proposed non-orthogonal eigen scheme.

Revisions in manuscript:

We have added the relevant statements in **lines 207 - 209** in the revised manuscript.

Comment: (7) Line 208 and Line 234: the RMSE of the same parameters should be given to allow comparison.

Response: Thank you for this valuable comment. Following the reviewer's advice, we have uniformly use elliptical Stokes parameters and its RMSE to describe and evaluate the accuracy of output polarization states. We have re-calculated the simulated and measured elliptical Stokes parameters of the target output states under various incident angles ranging from -60° to 60°, and updated the corresponding statements in revised manuscript.

Revisions in manuscript:

We have re-measured the fabricated samples under tilting incident angles within [-60°, 60°], and the corresponding RMSEs in simulated and measured Stokes parameters are placed in **lines 253 – 257** in the revised manuscript.

Comment: (8) Fig. 2E: it is hard to interpret the data in these plots without a reference for baseline and units / 2 pi.

Response: We thank for this meaningful suggestion for a clear figure illustration. We have added the baseline for each amplitude and phase profiles of eigen-values, and changed the unit / 2π for phase scales in the revised Fig. 2E.

Comment: (9) Fig. 3A: the dashed line is hardly visible anywhere, its color could be changed.

Response: Thank for your advice on the indiscernible dashed lines in Fig. 3A, we have changed the color of the ideal output states to uniform grey and the color for simulated ones to a variable colormap, and changed thicknesses of ideal and simulated results differently in the revised Fig. 3A.

Comment: (10) Fig 3C: a color plot with a color map reduced to [0.8, 1] would be easier to read.

Response: We totally agree with reviewer that Fig. 3C with a colormap scale of [0.8, 1] would be more readable, and we have added a colormap to label different values of specific efficiency values in Fig. 3C in the revised manuscript.

Comment: (11) Fig. 4C: it should be xy plane instead of xoy plane if z is not 0.

Response: Thank you for this kindly reminding. We have changed all labels of "xoy" to "xy" plane, and correspondingly indicated the specific propagation distance *z* in the revised manuscript and SI.

Comment: (12) Fig. 4D: the data would be more readable if the plot resembled Fig. 3D.

Response: Thank you for this kindly suggestion. We have re-organized Fig. 4D within 2D histogram similar to that of Fig. 3D.

Comment: (13) I have not found a picture of the goal intensity profiles of the number-dot holograms.

Response: Thank you for this comment. Due to the limited space in main text figures, we have displayed the goal intensities of number-dot holograms in Fig. S24 in SI.

Comment: (14) The spelling of words starting with eigen sometimes uses a dash, a space, or no space. This should be harmonized.

Response: We are grateful for this kindly suggestion. We have uniformly added a short dash "-" between eigen and its following words, including eigen-values, eigen-vectors, eigen-formalism, and so forth.

Comment: (15) The manuscript lacks some articles, the authors use constrain but I believe it should be constraint.

Response: Thank you for kindly advising on English and language mistakes. We have revised such improper usages according to the specific statements. Besides, we have tried our best to polish the language and re-checked all other similar situations in the revised manuscript.

Reviewer #3 (Remarks to the Author):

General comment: The authors introduced a framework to use the non-orthogonality of eigenstate pairs of non-Hermitian Jones matrices to achieve any polarization transformations. They used multilayered metasurfaces to relax the requirement for orthogonality between polarization eigenstates, resulting in efficient and broadband polarization transformations. The capabilities to enable gating and independent modulation in quadplex transmitting channels were also demonstrated. But we have some concerns to be addressed before considering publication.

Response: We are grateful for your constructive comments, and we have tried our best to address the problems and make corrections. We hope the revised version can be further considered for publication.

Comment: (1) The authors mentioned that non-orthogonal metasurfaces can be used to achieve arbitrary input-output polarization modulations in a broadband and angle-insensitive manner. The authors should explain what "angle-insensitive" means in this context. Does it refer to the incident angle or other angles? It seems that there is no result or data provided to prove that the discussed system is truly angle-insensitive. I suggest the authors to provide more details to support the conclusion of "angle-insensitive manner".

Response: The proposed "angle-insensitive" manner indicates the proposed input-output polarization conversion is insensitive to the incident angle. In our work, we have simulated and measured the non-orthogonal metasurface samples under illumination of incident angles within [-60°, 60°], and the corresponding efficiencies for target input-output polarization conversions are displayed in Fig. 3F and 3G. The average measured efficiency can reach 90% within incident angle ± 45°, and slightly decreases to 87% for incident angle from 45° to 60°. Meanwhile, taking 11# metasurface as a representative prototype, the corresponding simulated and measured output polarizations are displayed on Poincaré sphere (inset of Fig. 3F and 3G). To evaluate the precise of output polarization states with incident angles ranging from -45° to 45°, the measured RMSEs in Stokes parameters are 0.03 and 0.07 (S_1), 0.13 and 0.16 (S_2), 0.07 and 0.08 (S_3), respectively. Thus, based on these observations of efficiency and precise output polarization shape, we termed this as the "angle-insensitivity" manner of proposed non-orthogonal metasurfaces against tilting incident angles within [-45°, 45°]. As suggested by reviewer, we have added the specific explanations and strict range limitation [-45°, 45°] of "angle-insensitivity" in the revised manuscript.

Revisions in manuscript:

We have added the explanations and analyses on "angle-insensitivity" in **lines 253 – 257** in the revised manuscript.

Comment: (2) The authors should provide more details on the experimental setup of the gating of CP channels and independent hologram manipulations for reproducibility. In addition to considering the phase compensation for the target image, it is necessary to consider the phase difference of incident waves in a metasurface-based hologram. I suggest to clarify if there is a specific angle for the incident wave. Is the incident wave a uniform plane wave or a Gaussian wave? The phase and amplitude spectra of the S parameters for non-orthogonal metasurfaces should also be given, as they are the critical parameters for metasurface-based hologram.

Response: Thank you for this professional comment. Here, we would like to specifically explain the detailed measurement processes, especially for incident wave installation, and additionally to supplement the relevant S parameter simulations and measurements in the revised manuscript.

(i) *Details on experimental setups for CP gating and hologram.*

This experiment involving CP holographic imaging has been conducted as near-field measurement in anechoic chamber, as schematically shown in Fig. S14b in SI. The Agilent 8722ES vector network analyzer (VNA) is used to record the complex transmission field information (S_{21} parameter), including both amplitude and phase responses of each polarization component. A 2 GHz - 18 GHz dual circularly polarized wideband horn antenna is used as the feeding source to launch the quasi-plane waves by setting the distance relative to the metasurface to more than $20\lambda_0$. Meanwhile, we adopt a fiber optic active antenna with an ultrasmall purely dielectric head of 6.6 × 6.6 mm^2 as receiver end to collect the transmitted electric field information. The probe receiver is fixed on two translation stages controlled by a motion controller and its position is incremented by a step of 2 mm. Thus, the probe receiver controlled by the motion controller could collect the output electric field information covering the whole detection *xy* plane at specific propagation *z* distance. Here we set the range of detection region the same as the preset imaging size (about $10\lambda_0 \times 10\lambda_0$), with focal distance $z = 5\lambda_0$. The receiver fiber probe can be conducted along horizontal and vertical directions to collect *x*- and *y*-linearly polarized fields, i.e., E_x and E_y components. Thus we can further perform transmission electric fields for left- and right-handed circular polarizations as $E_L = E_x + iE_y$ and $E_R = E_x - iE_y$, respectively. Through combining different polarizations of source antenna (LHCP and RHCP), the quadruplex transmission field components in circular polarization base can be measured, including *L*-output under *L*-input, termed as complex component T_{LL}, the *R*-output under *L*-input as T_{RL}, the *L*-output under *R*-input as T_{LR}, and the *R*-output under *R*-input as T_{RR}. As a result, we are able to obtain the complex electric distribution in the whole imaging region, and the CP gating effects and imposed holograms can be intuitively calculated through energy intensities and phase distributions. Besides, for a clear illustration for the conducted experiments in our work, we listed the detailed setups for arbitrary input-output polarization conversion and holographic imaging detection measurements in following table.

Table. R2 Different experimental setups

		Arbitrary polarization conversion	**Near-field hologram imaging**
Source end	Transmitting device	Horn antenna	Horn antenna
	Polarization mode	Dual linear polarizations *x*- & *y*-	Dual circular polarizations LHCP & RHCP
	Illumination method	Normal & oblique	Normal

	Distance to sample	> $20\lambda_0$	> $20\lambda_0$
Analyzer		Agilent 8722ES vector network analyzer (VNA)	
Receiver end	Receiving device	Dual linearly polarized horn antenna	Dual linearly polarized fiber probe
	Polarization mode	Dual linear polarizations x- & y-	Dual linear polarizations x- & y-
	location	Local point Aligning to sample center	Global imaging region Scanning range $10\lambda_0 \times 10\lambda_0$
	Distance to sample	> $100\lambda_0$	= $5\lambda_0$

(ii) *Installation for incident waves.*

To answer the question from reviewer firstly, the incident wave is arranged so as to behave as a uniform plane wave. We also set the light impinging at normal incidence on the holograms for the projection experiments. In experiment, we use a 2 GHz - 18 GHz dual circularly polarized wideband horn antenna as the feeding source. To obtain the uniform output wave-front, we set the distance between source antenna and the sample more than $20\lambda_0$ to mimic the quasi-plane normal incident wave according to the antenna theory. However, as mentioned by reviewer, the wave-front of horn antenna is not fully plane wave, which would inevitably affect the output hologram projection. Accordingly, the measured energy intensities of four representative metasurface samples are shown in Fig. 4c, where the holographic characters "1", "2", "3", "4" imposed in different gated channels can be obviously distinguished. Although the measured holograms are deteriorated to some extent compared to the ideal imaging, partly due to the quasi-plane illumination, the gating effect and phase-modulated functionality have been successfully verified.

(iii) *S parameters for non-orthogonal metasurfaces.*

Following the suggestion from reviewer, we added the S parameter simulations of representative non-orthogonal meta-atoms adopted for holographic metasurfaces construction, as shown in Fig. R3. For $\boldsymbol{C}_4^1$ gating on L-L channel, the amplitude and phase responses of the 12 adopted meta-atoms are displayed in Fig. R3A. High degree of contrast for transmission coefficient between selected channel (L-L) and other three suppressed channels (R-L, L-R and R-R) are observed, and the corresponding phase responses of the meta-atoms in L-L channel can achieve the whole 2π coverage. When two L-L and R-L channels are both selected for $\boldsymbol{C}_4^2$ gating, both amplitudes of $|F_{LL}|$ and $|F_{RL}|$ are obviously over that of $|F_{LR}|$ and $|F_{RR}|$, as shown in Fig. R3B. Phase responses $\angle F_{LL}$ relies on propagation phase scheme that covers 2π for hologram generation, and $\angle F_{RL}$ is the primary response which can be further supplemented by geometric phase to perform the required phase distribution in R-L channel. For $\boldsymbol{C}_4^3$ gating effect, we adopted 16 meta-atoms for construction and the corresponding responses are displayed in Fig. R3C. Notably, the contrast degree in selected three channels and suppressed one is not as distinct and uniform as previous two cases, due to the increased phase requirements for producing three independent holograms. Under this restriction, $\angle F_{LL}$ profile can still support 2π coverage, while the primary cross-polarized phase responses in R-L and L-R channels also cover 2π by geometric phase for independent holograms. Fig. R3D shows the S parameters of metasurface for $\boldsymbol{C}_4^4$ with full quadruplex holograms, whose average amplitudes are 0.57, 0.50, 0.50, 0.52, respectively, and four phase profiles can independently cover 2π by adopting chirality-assisted phase, propagation phase, and geometric phase.

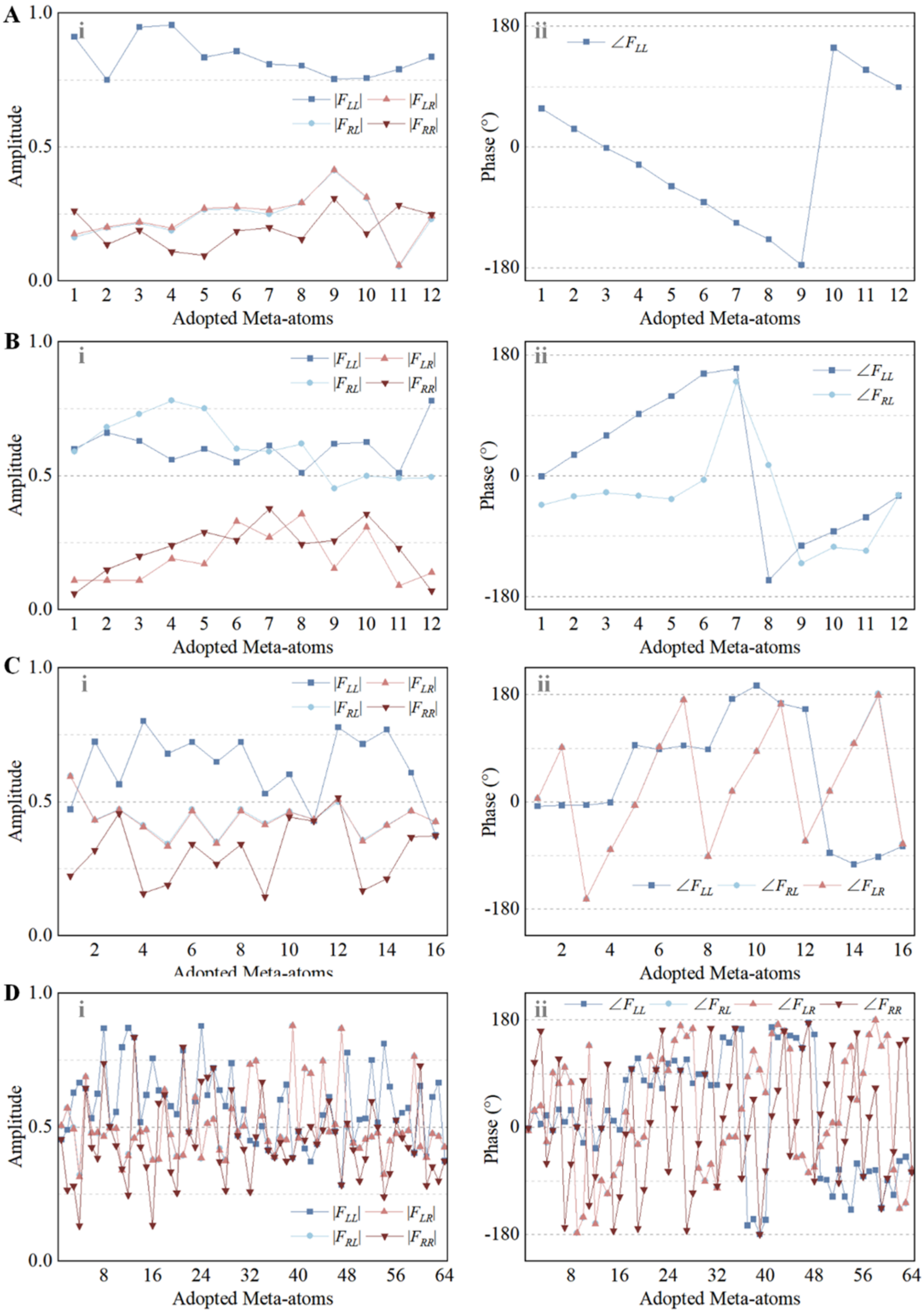

Fig. R3 (Fig. S25) Simulated S parameters of adopted meta-atoms for non-orthogonal metasurfaces constructions with (A) $\boldsymbol{C}_4^1$ for L-L channel, (B) $\boldsymbol{C}_4^2$ for L-L and R-L channels, (C) $\boldsymbol{C}_4^3$ for L-L, R-L and L-R channels, (D) $\boldsymbol{C}_4^4$ for full channels, respectively. (i) amplitude and (ii) phase responses at operation frequency 10 GHz.

Revisions in manuscript:

(i) We have added the detailed introductions on experimental setups for gating of CP channels and independent holograms detections in **Note 7.3** in the revised supplementary information.

(ii) We have specifically illustrated the setups for incident sources and discussed the impacts of quasi-plane waves on the output holograms in **Note 10.5** in the revised supplementary information.

(iii) We have added the phase and amplitude spectra of the S parameters for four representative non-orthogonal metasurfaces in **Note 10.4 and Fig. S25** in the revised supplementary information.

Comment: (3) In the measurement of the near-field distributions, a probe was used as the receiver. Generally, a probe can only measure the electrical field at a localized point in space, making it difficult to accurately measure the response of left-handed or right-handed polarized waves. More details should be given to demonstrate how to use the probe to measure the holographic images under different circular polarization excitations and why a circularly polarized horn is not used as the receiving antenna.

Response: We are grateful for this comment on our experiments on circularly polarized measurements. **We take a fiber probe with an ultrasmall purely dielectric head of 6.6 × 6.6 mm^2 as the receiving end, due to its portability and movable abilities, and negligible field perturbation (details in *http://www.enprobe.de/datasheets/EFS-105.pdf*).** As specifically stated in the previous reply to comment 2, a probe can be conveniently driven by a motion controller to scan the global imaging region perpendicular to the propagation direction. Under the circularly polarized incident waves, the transmitted electric fields E_x and E_y components can be collected using the receiving probe along horizontal and vertical directions. Thus, output circular polarizations can be calculated by $E_L = E_x + iE_y$ and $E_R = E_x - iE_y$, and quadruplex CP energy intensities and phase distributions for required holographic imaging can be obtained. Comparably, there are three primary reasons for not choosing a horn antenna as the receiving end. First, the circularly polarized horn antenna in X-band is bulky to be moved. Second, the aperture of horn is too large for collecting field information at precise location on the target *xy* plane. Finally, metallic structure of horn antenna would produce inevitable reflections and scatterings during the measurement. Thus, we chose a fiber probe as the receiver for near-field detection measurement. We thank reviewer again for this valuable comment, and we have added the analyses on data processing in the revised manuscript and SI.

Revisions in manuscript:

We have added the details on mechanism of detection probe in experiments, and explained the methods for circular polarization detection and transformation in **Note 4** in the revised supplementary information.

Comment: (4) In Fig. 3E, the measured polarization conversion efficiency of the metasurface samples is very high in the bandwidth of 8 GHz-12 GHz. However, in Figure 4E, why does the bandwidth reduce to 9 GHz-11 GHz?

Response: We thank reviewer for this comment. In the previous version, we have organized Fig. 4E to display the measured correlation coefficients of each produced hologram in the selected channels. This correlation coefficient is calculated from the experimentally measured and ideal images, which is utilized to express the level of similarity between produced and calculated ideal holograms. We see that for different gating requirements, the measured correlation profiles in the selected channels are obviously higher than those in suppressed channels around the operation frequency of 10 GHz. Meanwhile, the correlation coefficients for measured imaging qualities are degraded when deviating from the target frequency, and the degree of contrast between gated and suppressed channels are also deduced. <u>To properly analyze the performance of our holographic projection, we retrained our measurement within 9 GHz - 11GHz bandwidth, instead of the whole X-band in microwave region.</u> Nevertheless, the correlation properties sufficiently prove the multiplexing and gating abilities of non-orthogonal metasurfaces, and also reveal the dispersion effects associated to the phase-engineered holograms.

Comment: (5) There are many existing orthogonal metasurfaces that can reach a 100% polarization conversion efficiency in a wide bandwidth, such as PB-phase metasurfaces. The authors should further discuss the performances or functionalities that cannot be achieved by these orthogonal metasurfaces but can be offered by the proposed non-orthogonal metasurfaces.

Response: Thank you for this suggestion for us to compare our non-orthogonal metasurface with classical orthogonal metasurfaces. In our work, the “orthogonal” and “non-orthogonal” metasurfaces are referred to their eigen-states are orthogonal to each other or not. As mentioned by reviewer, the PB-phase metasurfaces are classical orthogonal case, whose eigen-states are orthogonal linear polarizations along the fast- and slow-axes of adopted meta-atom. The 100% polarization conversion of PB metasurface are strictly limited within two conditions. One is the π phase retardation between orthogonal linear eigen-polarizations, guaranteeing the complete conversion from input circularly polarized state to the corresponding cross polarized output state. The other restriction is the 100% conversion can only be conducted between pure circular polarizations, owning no applicability to other arbitrary elliptical polarization. Except for PB-phase metasurfaces, there also exist lots of metasurfaces to perform polarization conversions. For instance, Huygens’ metasurface and impedance surfaces are studied to optimize the efficiency performances of polarization conversions, but almost limited to linear polarizations and narrow bandwidth [33]. A novel topology-optimized metasurface is proposed recently to achieve the arbitrary polarization conversion, while its eigen-scheme still limited to orthogonal elliptical states, and the efficiency and bandwidth performances are not discussed [31]. In contrast, **our non-orthogonal metasurface owns several advantages that orthogonal cases are not able to perform**:

(i) <u>*For mechanism*:</u> Through breaking the orthogonality limitation between eigen-states, the matching Jones matrix models would be boosted to perform the near-unity efficiency properties. Except for the single-input to single-output arbitrary polarization conversion, the abundant capabilities held by non-orthogonal eigen-formalism can further provide extra degree of freedoms to achieve multiple-input to multiple-output polarization multiplexing and phase modulations.

(ii) *For performance*: In our work, the non-orthogonal metasurface is demonstrated to have the required universal adaptability to arbitrary elliptical polarization conversion with high performances, including high efficiency, broad bandwidth, and incident angle-insensitivity. Besides, we have also verified in the SI that our proposed non-orthogonal eigen-formalism can be applied in other wavelength regimes, including in the visible and IR regime (600 nm and 1550 nm), with appropriate meta-atom configurations.

As suggested by reviewer, we have added the discussions on advantages of our non-orthogonal metasurfaces to classical orthogonal metasurfaces in the revised manuscript.

Revisions in manuscript:

We have briefly discussed the comparisons between classic orthogonal metasurface and our proposed non-orthogonal metasurfaces in **lines 56 – 59** and re-emphasized on the advantages of our non-orthogonal scheme in **lines 66 -70** in the revised manuscript.

Other minor concerns:

Comment: (1) Line 57, "the center (7))" should be corrected to "the center (7)"

Response: We are sorry for this mistake. We have revised it and re-check the whole text about similar mistakes in the revised manuscript.

Comment: (2) Line 253, "selected threshold as |F| > 0.7 and suppressed threshold as |F| < 0.1," please give the definition of |F|.

Response: Thank you for this kindly reminder. The definition of |F| is the amplitude of transmission coefficients of circularly polarized channels, including L-L, R-L, L-R, and R-R channels, which has been specifically explained in the revised manuscript.

Revisions in manuscript:

We have added the explanations on |F| in **lines 271– 275** in the revised manuscript.

Comment: (3) Line 264, "Under normal illumination of LHCP or RHCP beams propagating along +z-axis," please add the corresponding Cartesian coordinate in Fig. 4B.

Response: Thanks for this suggestion. We have added the Cartesian coordinate in Fig. 4B in revised manuscript.

Comment: (4) The resolution of figures is a bit low, please improve them.

Response: We thank you for this comment, we have improved the resolution of all figures with (or higher than) 300 dpi × 300 dpi.

Reviewer #4 (Remarks to the Author):

I co-reviewed this manuscript with one of the reviewers who provided the listed reports. This is part of the Nature Communications initiative to facilitate training in peer review and to provide appropriate recognition for Early Career Researchers who co-review manuscripts.

Response: We gratefully thanks for the precious time you have spent on making such constructive comments. All the suggestions and comments are carefully replied and listed in the about response parts. We are really grateful for your further consideration about our work.

REVIEWERS' COMMENTS

Reviewer #1 (Remarks to the Author):

The authors have addressed all the concerns and queries in my last report. I am happy to recommend its publication in Nature Communications.

Reviewer #2 (Remarks to the Author):

Second Review for "Reaching the Efficiency Limit of Arbitrary Polarization Transformation with Non-orthogonal Metasurfaces" by Yueyi Yuan et al.

The authors have considerably increased the readability of the manuscript and the quality figures. The error bars in Fig. 3E are reasonable now. The authors also answered my questions in their extensive rebuttal. The manuscript is still a steep step into polarization for a non-specialist, but the other reviewers have not mentioned so this is probably a personal impression. I think the manuscript can now be published in Nature Communications.

Minor Comments

Line 49: a character reads wrong in the equation

Line 257: should it be [-60deg, 60deg]?

Reviewer #3 (Remarks to the Author):

The authors have made good revisions according to our comments and suggestions, including adding specific steps for experimental testing to enhance the reproducibility of the work. The phase response curve of the metasurface unit has also been added, proving that the designed metasurface unit can cover 360 degrees in the phase response. We have no further revision suggestions.

Reviewer #4 (Remarks to the Author):

All my concerns have been well addressed.